SCIEPublish

Review

Photocatalytic Antifouling Coating: From Fundamentals to Applications

Wenhui Bian [1], Huaicheng Li [2], Wei Xiong [1,2,*] and Michael K. H. Leung [2,*]

[1] Key Laboratory of Industrial Ecology and Environmental Engineering (Ministry of Education), School of Environmental Sciences and Technology, Dalian University of Technology, Dalian 116024, China; 13504691059@163.com (W.B.)

[2] Ability R&D Energy Research Centre, School of Energy and Environment, City University of Hong Kong, Kowloon Tong, Hong Kong, China; richalee4-c@my.cityu.edu.hk (H.L.)

* Corresponding author. E-mail: xiongwei@dlut.edu.cn (W.X.); mkh.leung@cityu.edu.hk (M.K.H.L.)

Received: 25 July 2024; Accepted: 10 October 2024; Available online: 14 October 2024

ABSTRACT: With the rapid development of shipping industry, marine vessels frequently suffer from biofouling caused by marine organisms, making the effective prevention of marine biofouling a critical issue. Traditional antifouling coatings, which utilize toxic and harmful substances, pose significant risks to marine ecosystems. Therefore, the development of environmentally sustainable antifouling coatings has become imperative. Photocatalytic antifouling coatings, as an eco-friendly alternative, present a promising solution to these economic, energy, and ecological challenges. This review compares the environmental benefits of photocatalytic antifouling coatings to traditional ones, highlighting the underlying mechanisms of marine biofouling. Additionally, it explores the preparation techniques employed in photocatalytic antifoulant, analyzing the advantages, disadvantages, and potential modifications for photocatalytic coatings. Based on these insights, the future development of photocatalytic antifouling coatings is discussed, aiming to provide valuable references for the exploration of more efficient, broad-spectrum, energy-saving, environmentally friendly, and cost-effective marine antifouling technologies.

Keywords: Biological fouling; Antifouling coatings; Photocatalysis; Environmental benefits

1. Introduction

With the rapid development of the shipping industry, marine vessels are increasingly affected by biofouling caused by marine organisms such as bacteria, diatoms, barnacles, and shells [1]. These fouling organisms readily attach to the surfaces of ships, pipelines, aquaculture cages, leading to metal corrosion, shortened service life and heightened safety risks. Additionally, biofouling increases navigation resistance, which in turn elevates energy consumption, and subsequently raises greenhouse gas emissions [2,3]. Furthermore, biofouling can result in biological invasions when non-native species attach to ship hulls and are transported to new environments, thereby threatening local marine ecosystems [4]. The economic burden of marine biofouling on the maritime industry is substantial, amounting to an estimated $150 billion annually, highlighting its significant economic, environmental, and safety impacts [5].

Biofouling in the ocean follows a the linear succession model, occurring in three main stages (Figure 1) [6]. Initially, organic matters such as polysaccharides and proteins rapidly deposit on equipment surfaces through physical adsorption mechanisms (like van der Waals forces, Brownian motion, electrostatic attraction, etc.), forming a conditioning film. Within 24 h, bacteria, diatoms, and other microorganisms adhere to this film, utilizing macromolecular nutrients and secreting extracellular polymers (e.g., hyperg lycans, glycoproteins, lipids) to create a biofilm. Subsequently, larger fouling organisms such as algae, hydrozoa, and barnacles attach to the biofilm within a few weeks, forming complex biological communities [7,8]. The extent of marine fouling depends on factors such as the duration and cruising speed of ships, seasonal variations, and water characteristics in different regions [9]. However, biofouling does not always occur in this strict sequence, as some marine species (e.g., zoospores of *Ulva linza*, cyprids of *Amphibalanus amphitrite*)

https://doi.org/10.70322/prp.2024.10008

may simultaneously attach to equipment surfaces [10,11]. While the fouling pattern is consistent across regions, the dominant species generally differ [5].

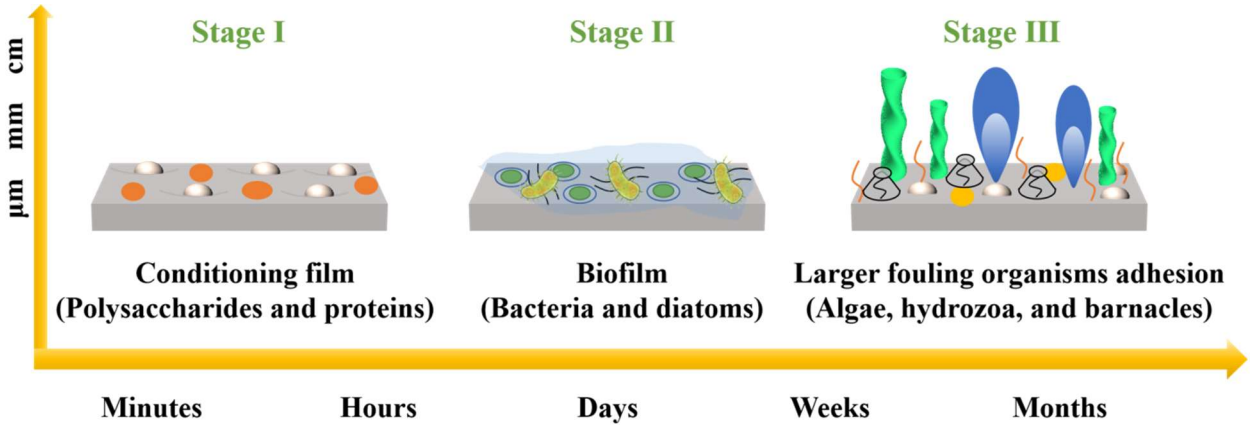

Figure 1. Schematic diagram of the biological fouling process.

To mitigate marine biofouling, antifouling coatings are commonly employed as an effective preventive measure. Traditional antifouling coatings include dissolving, contact, diffusion types. Regardless of the type, traditional antifouling coatings often lead to marine environmental pollution and ecological damage. It is attributed to the biocides typically used to kill fouling organisms, which can also harm non-target marine species, affect their reproductive systems, and, in severe cases, lead to population extinction. To address the ecological risks and microbial resistance associated with traditional antifouling coatings, novel antifouling coatings have been developed, including fouling release coatings, photocatalytic antifouling materials, natural antifouling agents derived from biomimetic strategies, micro/nano structure antifouling materials and hydrogel antifouling coatings [12]. These non-toxic antifouling technologies emphasize the principle that "prevention is better than cure" and need to be evaluated for both acute and chronic ecotoxicity [13].

Recently, photocatalytic antifouling technology has emerged as a promising solution to marine biofouling, offering adaptability to complex marine environments and reducing environmental pollution. Titanium dioxide (TiO_2), a well-studied photocatalyst for over a century, has been extensively researched for its bactericidal effects on viruses, bacteria, and algae since the 1970s [14]. TiO_2 is favored for antifouling applications due to its strong photocatalytic activity, low cost, and stable chemical properties [15]. Current research focuses on optimizing the physicochemical properties of TiO_2 through various modification methods to enhance its catalytic activity and visible light utilization efficiency, including broadening the absorption wavelength range [16], improving light energy utilization efficiency [17] and promoting photogenerated carrier separation [18]. By integrating multiple modification processes, the antifouling capabilities of photocatalytic coatings can be significantly enhanced, reducing the reliance on chemical reagents and leveraging solar energy to lower overall energy consumption [19].

While most literature on marine antifouling focuses on the development of new polymers, comprehensive reviews of photocatalytic antifouling agents are relatively scarce. This review aims to summarize the preparation and modification of photocatalytic antifouling agents and explore strategies for enhancing their photocatalytic activity. Additionally, the mechanisms and future development of photocatalytic antifouling coatings will be discussed, providing insights into potential advancements in efficient, broad-spectrum, energy-saving, environmentally friendly, and cost-effective marine antifouling technologies.

2. Fundamentals of Photocatalytic Antifouling

2.1. Mechanism of Traditional Antifouling

The development of antifouling coatings has spanned centuries [20]. In the era of wooden ships, the hulls were protected from biofouling by covering them with metals such as lead and copper or by coating them with hot asphalt, tar, and grease [21]. By the 17th century, antifouling technology had advanced to using rosin loaded with cuprous oxide or insecticides to release toxic substances into seawater, effectively killing or repelling marine biofoulings. In the latter half of the 20th century, tributyltin (TBT) self-polishing antifouling coatings became widely used for their effectiveness. These coatings continuously released organotin compounds when exposed to seawater, providing robust antifouling protection for up to five years [9,22]. However, TBT poses significant environmental hazards. Once introduced into the

marine ecosystem, it degrades slowly through microbial and photolytic processes. It bioaccumulates in marine organisms such as gastropods, bivalves, and fish. Additionally, it also easily adsorbs onto suspended particles due to its hydrophobic properties, eventually settling into sediments where it degrades over several years to decades [23,24]. TBT is considered one of the most dangerous chemical ever released into the environment by human beings, affecting the growth, development, and reproduction of marine organisms and posing serious threats to human health [25]. Due to its high persistence and non-selective toxicity, TBT is recognized as one of the most harmful pollutants to marine ecosystem. Consequently, the International Maritime Organization (IMO) bans the production of TBT-containing antifouling coatings in 2003 and bans their use globally in 2008 [26,27]. However, residual TBT remains in marine environments, continuing to negatively impact biological communities [28]. Following the prohibition of TBT, copper (Cu) re-emerges as a widely used and effective antifouling agent. Copper compounds in antifouling paints oxidize to Cu^{2+} in the oxygen-rich seawater, providing antiseptic and bactericidal properties. However, their effectiveness is relatively short-lived, necessitating frequent cleaning and repainting of ships and equipment [29]. Once released, Cu ions undergo various processes, including adsorption on solid surfaces, absorption by organisms, precipitation as solids, and complexation with dissolved ligands, all of which affect their formation, mobility, and toxicity [30]. While Cu is an essential trace element and less toxic than TBT, its accumulation in the ocean can increasingly impact marine ecosystems [31]. Due to the lack of ideal alternatives, Cu-based antifouling coatings are still in use.

Additionally, other compounds such as Irgarol 1051, benzamide, chlorothalonil, dichloroside, diazuron, and zineb are commonly employed as antifouling agents, although they are also regulated due to their marine hazards [20,32,33]. The prohibition of toxic and harmful fungicides worldwide has promoted the development of antifouling coatings towards sustainable and non-toxic alternatives. Additionally, electrochemical technology has long been used to prevent the attachment of marine organisms on underwater structures. Gaw et al. developed an electrochemical system with dual antifouling and antibacterial functions, using short square wave pulses to induce water reduction and inhibit bacterial adhesion [34]. This approach introduced a novel concept for electrochemical antifouling. Conductive coatings incorporating carbon-based additives, modified carbon, and metals have been investigated for various electrochemical antifouling applications, serving as electrode materials on ship hulls and other marine components to combat biofouling [35]. Both cathodic [36] and anodic currents [37], as well as alternating currents [38], can be employed in conductive coating, applying a voltage higher than the water decomposition threshold, which creates pH stress in the surrounding water layer, thus preventing organism attachment. However, electrolytic antifouling technology has certain limitations, requiring technical support and regular maintenance to ensure the efficient operation of the electrolytic system. Many animals and plants in nature have evolved surfaces with excellent antifouling properties. Inspired by these natural antifouling surfaces, efforts have been made to develop coatings that mimic these properties (Figure 2) [39]. Inspired by the natural antifouling ability observed in certain marine organisms, researchers have explored the use of natural antifouling agents extracted from organisms such as cnidarians, ascidians, sponges, algae, and seagrass, which can effectively inhibit the growth and reproduction of fouling organisms [40]. Darya et al. utilized the bioactive extract of sea cucumber *Stichopus herrmanni* as a natural antifouling agent, following by combining this extract with the biopolymer polycaprolactone/polylactic acid to create an efficient biodegradable self-polishing antifouling coating [41]. Among nine bioactive extracts from different organs, the ethyl acetate extract from the body wall of sea cucumber had the highest antifouling activity, including superior antibacterial and anti-barnacle properties, and lower non-target biological toxicity. Recently, inspired by unique micro/nano structures on the surface of some animals and plants (such as whales, sharks, cicadas, lotus leaves, etc.), micro/nanostructured antifouling materials have been debeloped, mainly utilizing their microscopic structural morphology to inhibit the attachment of fouling organisms without harming the marine environment [42]. Guan et al. used the "flowering tree" microstructure found on mussel shells to prepare a biomimetic material, evaluating its resistance to diatoms [43]. This structure effectively prevented diatom attachment by not providing suitable attachment spaces. Moreover, the mucus secreted by the epidermis of certain fish can hinder the attachment of fouling organisms or promote their removal [44]. Hydrogels, which are soft and hydrophilic like fish skin mucus, can reduce the adhesion of proteins and polysaccharides due to their low surface energy, making them actively studied in marine antifouling. Yang et al. developed a hydrogel antifouling coating based on polyacrylamide-crosslinked multi-arm polyethylene glycol [45]. This coating, with an epoxy intermediate layer for strong adhesion, demonstrated excellent antifouling performance against proteins, polysaccharides, algae, and oils, and slowly degraded in seawater, facilitating the release of contaminants. Drawing inspiration from the Nepenthes pitcher plant, which uses a smooth, lubricated surface to catch prey, smooth liquid-injected porous surfaces (SLIPS) were created by injecting lubricants into substrates with micro/nanopores [46]. Inspired by the hagfish, which secretes mucus to evade predators, Tong et al. developed an intelligent SLIPS marine antifouling coating [47]. This coating featured responsive switching

lubrication modes and self-healing properties, facilitated by the interaction between azobenzene and α-cyclodextrin. The smart coating could switch between "enhanced" and "normal" antifouling modes depending on requirements, significantly extending its service life in marine environments. The material exhibited high efficiency in self-cleaning, and in resisting proteins, bacteria, and algae.

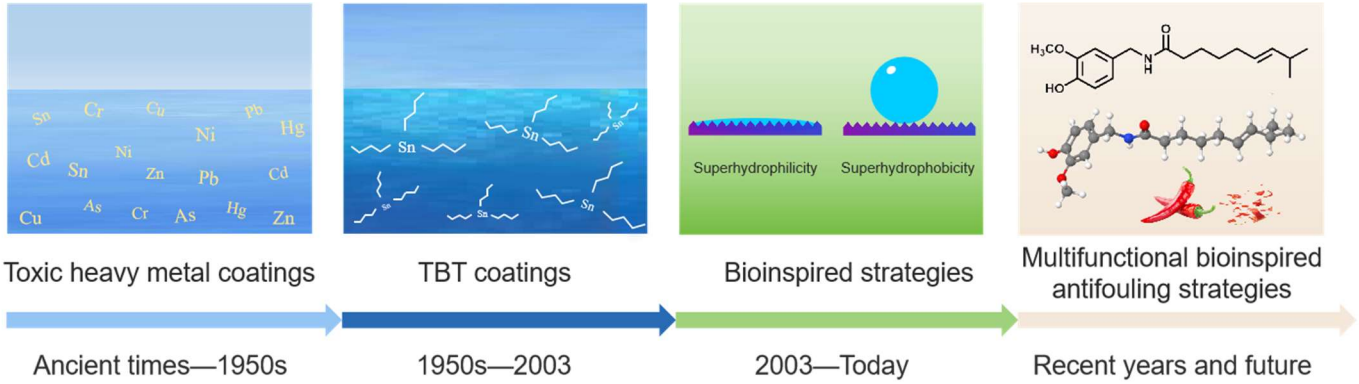

Figure 2. The development of antifouling coatings.

2.2. Antifouling Mechanism of Photocatalytic Technology

Photocatalysis refers to the process of utilizing solar energy to generate free radicals for the degradation of bacteria and organic matter through the action of a photocatalyst [48]. Compared to traditional technologies, photocatalytic antifouling technology selectively targets specific pollutants without releasing toxic substances that could harm other marine organisms, with the advantages of reusability, long-term stability, and environmental friendliness [49]. When semiconductor photocatalyst (such as TiO_2) are exposed to incident light with energy equal to or greater than their band gap, electrons in the valence band (VB) absorb energy and transfer into the conduction band (CB), resulting in the formation of positively charged photogenerated holes (h^+) in the VB and negatively charged photogenerated electrons (e^-) in the CB (Equation (1)) [50,51]. The h^+ exhibit strong oxidation capacity, while the e^- exhibit strong reduction capacity. These carriers react with H_2O and O_2 to produce reactive oxygen species (ROSs), such as hydroxyl radicals (•OH) and superoxide radical ($O_2^{\bullet-}$) (Equations (2) and (3)). These ROSs further react as intermediates to produce other ROS, such as singlet oxygen ($^1O_2$), hydrogen peroxide (H_2O_2), and hydroxyl peroxide (•OOH) (Equations (4)–(8)) (Figure 3) [52,53]. It is worth mentioning that •OH and $O_2^{\bullet-}$ have stronger antibacterial activity than $^1O_2$ and H_2O_2.

$$TiO_2 + h\nu \rightarrow e^- + h^+ \quad (1)$$

$$h^+ + H_2O \rightarrow \cdot OH + H^+ \quad (2)$$

$$O_2 + e^- \rightarrow O_2^{\bullet-} \quad (3)$$

$$h^+ + O_2^{\bullet-} \rightarrow {}^1O_2 \quad (4)$$

$$\cdot OH + \cdot OH \rightarrow H_2O_2 \quad (5)$$

$$e^- + O_2^{\bullet-} + 2H^+ \rightarrow H_2O_2 \quad (6)$$

$$O_2^{\bullet-} + H_2O_2 \rightarrow \cdot OH + OH^- + O_2 \quad (7)$$

$$O_2^{\bullet-} + H^+ \rightarrow \cdot OOH \quad (8)$$

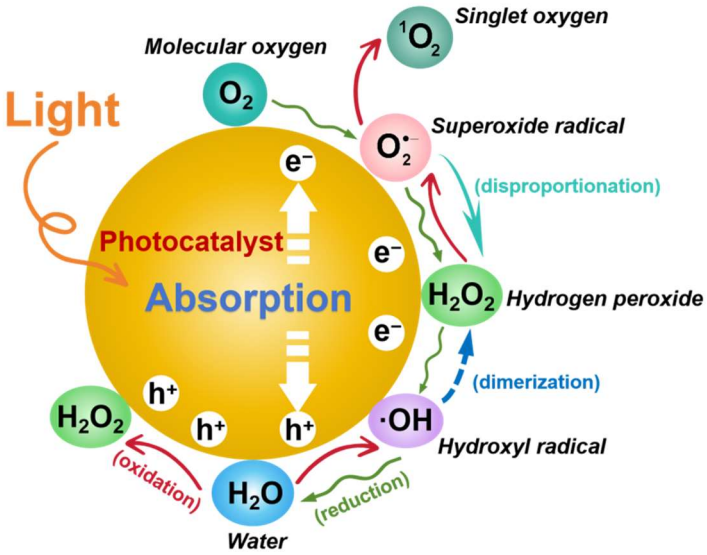

Figure 3. Schematic diagram of semiconductor photocatalysis.

ROSs produced by photocatalysis such as h^+, $O_2^{\bullet-}$, $^1O_2$, and •OH have short lifespans and require direct contact with microorganisms to exert their bactericidal effects, while H_2O_2 has a longer lifespans and can act without direct contact between the photocatalyst and microorganisms [54]. However, H_2O_2 preferentially interacts with microbial surfaces, which limits its decomposition [55]. These ROSs possess strong oxidation capabilities, enabling them to degrade lipids, polysaccharides, proteins, and other macromolecular organic substances rapidly, thereby destroying cell structures and killing bacteria and other microorganisms [56]. This environmentally friendly and energy-saving technology utilizes clean and renewable solar energy to address the issue of large-scale fouling biological attachment at the source, presenting a promising application in marine antifouling [57]. However, it is important to note that water significantly attenuates the intensity of ultraviolet light, reducing the effectiveness of the coating with increased depth, leading to more serious biofouling in less protected deeper structures. In addition, humus, a natural polymer widelypresent in natural water and its surrounding environment, has a strong adsorption and complexation ability, which can alter the light absorption intensity of water, thereby affecting the light absorption of photocatalytic antifouling coatings. Humus competes for light and photons, and may quench ROSs, thus affecting the activity of photocatalyst [58]. Furthermore, the performance of photocatalytic antifouling coatings is influenced by factors such as season and latitude [59]. To enhance the photocatalytic activity of these materials, extensive research is required. This includes addressing the recombination of electron-hole pairs in photocatalysts, expanding the light utilization rate, and improving the interaction between photocatalysts and reactants [60].

3. Recent Development of Photocatalytic Coatings

3.1. Photocatalytic Agents for Antifouling

Photocatalytic antifouling agents are generally classified into ultraviolet (UV) light-responsive and visible light-responsive materials. Their key distinction lies in the wavelength range of light they absorb and utilize for energy conversion. UV-responsive materials primarily harness UV light for photocatalytic reactions, while visible light-responsive materials are capable of utilizing light energy within the visible spectrum.

3.1.1. UV Light-Responsive Antifouling Materials

Many metal oxides are categorized as UV-responsive materials, with titanium dioxide (TiO_2) nanocrystals being extensively studied due to their ability to enhance the wettability and mechanical strength of coated surfaces. This, in turn, influences the interaction between marine organisms and the antifouling surfaces. TiO_2 naturally exists in three crystalline forms, namely rutile, anatase, and brookite. Among these, anatase is the most effective photocatalyst, while rutile is primarily used as a stabilizer in pigments or polymers [61]. Notably, a mixture of anatase and rutile exhibits superior photocatalytic performance compared to anatase alone [62]. With a bandgap of 3.2 eV, TiO_2 demonstrates excellent chemical stability and antifouling performance under UV light. Hu et al. successfully developed environmentally friendly TiO_2/polymer antifouling coatings by dispersing TiO_2 nanoparticles in water-based epoxy-modified tung

oil resin [15]. These coatings exhibited robust antibacterial activity under both light and dark conditions, with the synergistic effects of the polymer and TiO_2 offering protection against *Staphylococcus aureus* (*S. aureus*) and *Escherichia coli* (*E. coli*), while inhibiting the growth and adhesion of diatoms (*Cyclotella* sp.). Similarly, ZnO, which has a bandgap comparable to TiO_2, is another traditional photocatalytic agent. Laura et al. used electro-spraying to apply a photoactive sol-gel ZnO suspension coating to a glass substrate, creating a self-cleaning antibacterial surface [63]. The ZnO coatings exhibited photoinduced hydrophilicity and bacteriostatic effects, primarily due to photogenerated ROS and bioavailable Zn^{2+} from ZnO dissolution, remaining effective despite biofilm formation. The electro-sprayed surface achieved a bacteriostatic rate exceeding 99.9% against *S. aureus*. Cerium oxide (CeO_2), a rare earth metal oxide with a band gap of 2.8~3.1 eV, is also an effective UV-responsive material, which is characterized by low toxicity, low cost, large oxygen storage capacity and good stability. CeO_2-based photocatalysts, with their unique cubic fluorite structure, facilitate the reduction of photogenerated carrier recombination through easy transitions between Ce^{4+} and Ce^{3+} states, leading to abundant oxygen vacancies [64–66].

It is worth noting that the UV light accounts for only 4% of the total solar energy, while the visible spectrum comprises 43%, resulting in a low utilization efficiency of solar energy of these UV-responsive materials [67]. Additionlly, the high recombination rate of photogenerated electron-hole pairs in UV-responsive materials, further limits the potential applications in photocatalysis.

3.1.2. Visible Light-Responsive Antifouling Materials

It is well known that not all metal oxides are UV light-responsive materials. In particular, copper oxide (CuO), with its narrow band gap of 1.2~1.5 eV, is regarded as an effective visible light-responsive material for antibacterial application. CuO is abundant, inexpensive, photochemically stable, and biocompatible, which makes it an effective photogenerated electron acceptor and reduces recombination tendencies. Nano-sized CuO also exhibits superior hydrophobic properties compared to other metal oxides [68,69]. Similarly, Cu_2O nanoparticles (NPs) are widely used due to their high efficiency and broad-spectrum antibacterial properties. Sharma et al. demonstrated that copper-based NPs effectively kill *S. aureus*, *E. coli*, and other microorganisms. Smaller copper-based NPs, with their larger surface area, provided more interaction sites with microorganisms [70]. The IC_{50} values (the lowest concentration inhibiting 50% bacterial growth) for copper-based NPs were 200 μg mL^{-1} for *S. aureus* and 125 μg mL^{-1} for *E. coli*. The antibacterial activity was more effective against Gram-positive bacteria due to their thinner cell walls compared to Gram-negative bacteria.

Transition metal sulfides exhibit more suitable electronic structures and light response characteristics compared to large band gap metal oxides. CdS, with a narrow band gap (2.4 eV) and high visible-light activity, has significant redox potential and exists in cubic sphalerite and hexagonal wurtzite forms, with the metastable cubic phase transforming into the stable hexagonal phase upon heating [71–73]. Wang et al. prepared layered flower-like Au@CdS-CdS nanoparticles with a wide UV-VIS absorption range (850 nm), covering the entire visible range (400–760 nm), which significantly increased capture light [74]. The Au@CdS-CdS heterostructure improved the separation and transfer rate of photogenerated carriers, and the hierarchical structure provided more reaction sites.

Graphitic carbon nitride (g-C_3N_4) is a two-dimensional layered metal-free semiconductor with a band gap of approximately 2.7 eV. It is thermally polymerized from nitrogen-rich precursors and is highly stable against acids, bases, and organic solvents. The g-C_3N_4 is an abundant visible-light responsive photocatalyst, and its surface chemistry can be modulated at atomic and molecular levels through surface engineering, thereby reducing the photogenetated charge recombination, and improving the solar energy utilization efficiency [75,76]. Liu et al. prepared porous g-C_3N_4 ultrathin nanosheets with nitrogen vacancies by hydrochloric acid pretreatment of urea thermal polymerization [77]. These nanosheets exhibited effective inactivation of *S. aureus* and *E. coli*, demonstrating that nitrogen vacancies not only narrowed the intrinsic band gap of g-C_3N_4 but also introduced new defect states at the edge of the conduction band, expanding its visible light absorption range and enhancing photocatalytic activity. However, excessive defects might act as charge recombination centers, potentially lowering the separation efficiency of photogenerated charge carriers.

Bismuth-based photocatalysts, with suitable band gaps (mostly below 3.0 eV) and unique electronic configurations and layered structures, show excellent performance in photocatalytic antifouling. These include bismuth oxide, and bimetallic oxides (e.g., Bi_2WO_6, $BiVO_4$, Bi_2MoO_6), and bismuth oxyhalide (BiOX, where X = Cl, Br, I) being extensively studied [78,79]. Wu et al. found that the photocatalytic bactericidal activity of BiOBr nanosheets against *E. coli* under visible light irradiation depended on the main exposure surface [80]. BiOBr nanosheets with fully exposed {001} surfaces exhibited better photocatalytic activity than those with {010} surfaces, primarily due to higher photoinduced

carrier separation and transfer rates and more oxygen vacancies of {001} surfaces. By integrating ZIF-67, the novel Bi_2MoO_6/ZIF-67 S-scheme heterojunctions demonstrated high efficiency in visible light-responsive antifouling applications. When tested in a real marine environment, this photocatalyst showed excellent antifouling performance, significantly reducing the adhesion of microorganisms to surfaces [81].

Black phosphorus (BP), a two-dimensional layered non-metallic semiconductor, also exhibits visible light response. As a novel member of layered materials, BP features a large surface area, a band gap of 0.3~2.0 eV, high charge carrier mobility, and a long charge carrier diffusion path, making it a promising candidate for photocatalytic applications [82,83]. Liang et al. developed BP nanosheets doped with dense silver nanoparticles (AgNPs), finding that a lower concentration of Ag^+ facilitated the formation of smaller AgNPs (≈7 nm) (Figure 4A) [84]. BPNs-AgNPs seriously damaged the cell wall of *E. coli*, resulting in significant cytoplasmic leakage and high antibacterial activity, with antibacterial efficiency of 90% (Figure 4B). This BP-Ag nanostructure achieved enhanced antibacterial efficiency through the synergistic integration of the silver fungicide and the BP skeleton. The increased affinity of the nanosheets for bacteria promoted the co-inactivation of pathogens, showing excellent bactericidal effects across various bacterial strains. Additionally, the hybrid structure significantly improved photocatalytic efficiency by producing more efficient and stronger ROS (Figure 4C).

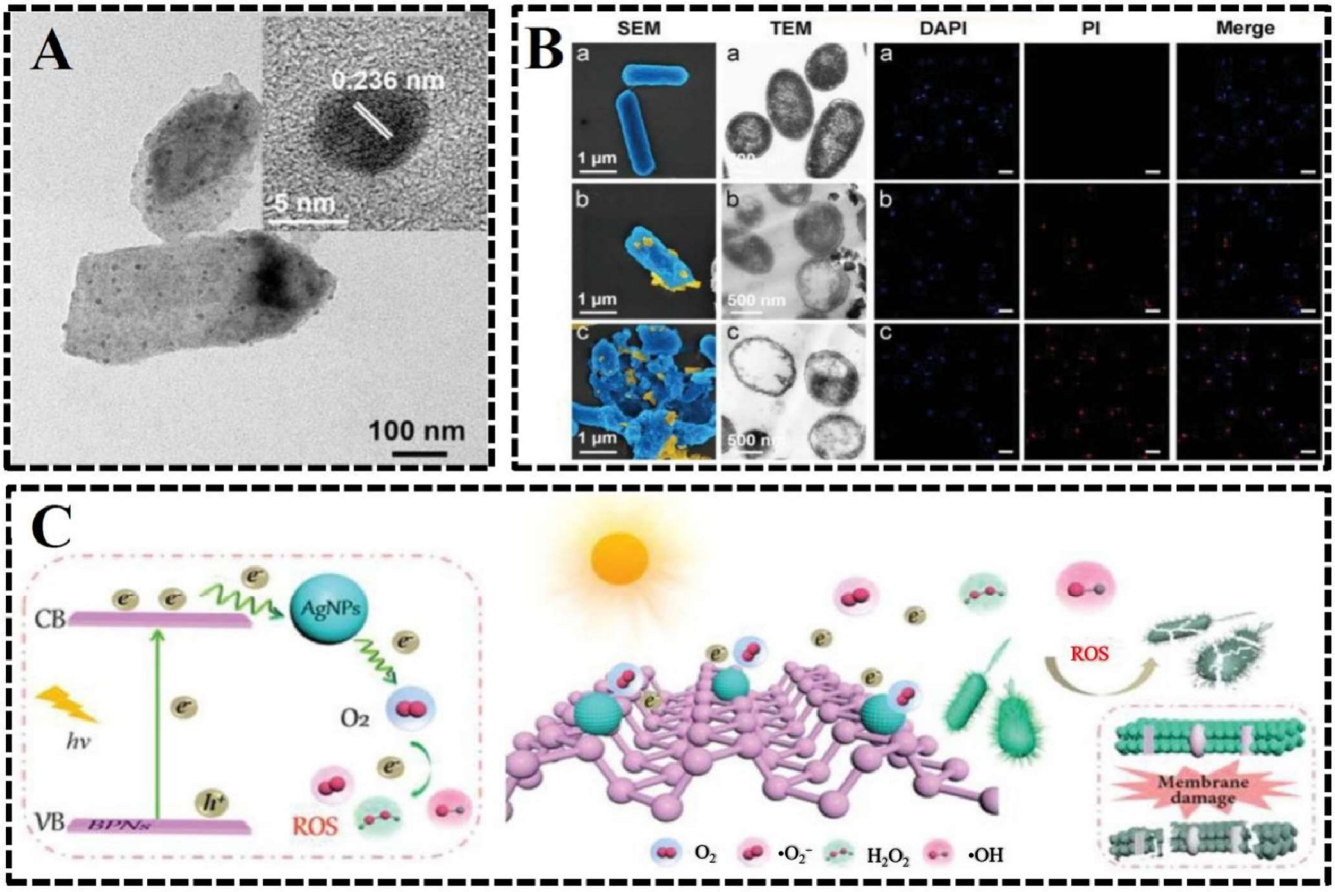

Figure 4. (**A**) TEM characterization of BPNs-AgNPs (7 nm); inset shows the corresponding highresolution TEM (HRTEM) image; (**B**) Membrane integrality characterization of (a) untreated *E. coli*, and treated with (b) BPNs and (c) BPN-AgNP nanohybrids by SEM, TEM, and fluorescence staining assay. The blue and yellow pseudo colors of SEM images were, respectively, utilized to mark the *E. coli* membrane and BPNs/BPN-AgNP nanohybrids according to their edge shape differences. Fluorescence images of *E. coli* were visualized by staining with DAPI (blue) and PI (red). Scale bar is 25 μm; (**C**) Schematic illustration of BPNs-AgNPs under light irradiation [84].

3.1.3. Regulation of Photocatalytic Agents

The aforementioned materials exhibit significant potential in the field of photocatalysis. However, several challenges hinder their practical application, including limited specific surface areas, low solar energy utilization efficiencies, and high recombination rates of photogenerated carriers. These issues pose substantial obstacles to the application of semiconductors in photodegradation processes. Various methods have been proposed to enhance their performance,

including morphology control, surface modification and electronic structure regulation [85]. Optimizing the morphology of photocatalysts not only enhances light absorption but also promotes the separation and migration of photogenerated charges by shortening transport distances. Additionally, it can also increase the specific surface area and enrich active sites, thereby enhancing surface catalytic reactions and accelerating photocatalytic reaction rates [86]. Xiang et al. prepared monoclinic $BiVO_4$ with various nanostructures by using different morphology control agents such as ethylenediamine tetraacetic acid, polyethylpyrrolidone, and sodium dodecyl sulfate [87]. Among these, $BiVO_4$ with a grape-like nanostructure demonstrated the highest photocatalytic bactericidal activity, achieving a sterilization rate of 99.9% within 120 min for *Pseudomonas aeruginosa* (*P. aeruginosa*), with h^+ as the main active species. Similarly, the photocatalytic and antibacterial properties of multifunctional $ZnWO_4$ NRs could be improved by controlling their size and crystallinity by the solvothermal process [88].

Another method to regulate light absorption is through the use of semiconductors with a narrow band gap or noble metal nanoparticles with surface plasmon resonance for surface modification [89]. The composite of two or more semiconductor materials forms a heterojunction structure, effectively broadening the optical response range of the involved semiconductors. Xia et al. synthesized a 0D/2D S-scheme heterojunction material by in-situ growth of CeO_2 quantum dots on the surface of polymerized carbon nitride nanosheets using a wet chemistry method [90]. In the S-scheme heterojunction system, two types of photocatalytic semiconductors are involved, namely oxidation type photocatalyst (OP) with positive valence band position and reduced type photocatalyst (RP) with negative conduction band position. In the absence of light, electrons from the RP flow into the OP, establishing an internal electric field at the RP-OP interface that prevents the continuous migration of electrons from the RP to the OP (Figure 5a). Under light irradiation, the internal electric field drives the photoelectrons in the CB of OP to consume the photogenerated holes in the VB of RP. Consequently, the CB of the RP and the VB of the OP accumulate photoelectrons and holes with enhanced redox capacity, resulting in a spatial separation of reduction and oxidation sites (Figure 5b). This S-scheme heterojunction material achieved a sterilization rate of 88.1% against *S. aureus* under visible light due to its effective utilization of photoinduced carriers and the generation of large amounts of active species. Sunida et al. prepared composite metal oxides containing TiO_2 and WO_3 (WO_3@TiO_2) using the sol-gel method [91]. These composite metal oxides demonstrated superior catalytic performance compared to mixed metal oxides prepared by the in-situ polymerization of TiO_2 and WO_3 particles with thiophene. The composite with 10 wt.% WO_3 (10% WO_3@TiO_2) exhibited the highest photocatalytic activity and is the most effective antifouling coating. In field tests of static immersion in seawater, the substrate covered with composite binder soaked in seawater for 30 days had the lowest CFU value (1.2×10^4) and the highest colony reduction rate (92.94%). Lv et al. synthesized g-C_3N_4 nanosheets modified with ZnO nanorods via chemical etching [92]. The ZnO-C_3N_4 heterostructure enhanced visible light absorption and prolongs the lifespan of photogenerated electron-hole pairs. Addressing the limitations of high surface energy and photogenerated electron-hole recombination significantly contributed to an inhibition rate of 100% against *Bacillus subtilis* within 8 h. Mao et al. synthesized a BiOI@CeO_2@Ti_3C_2 terpolymer photocatalyst by combining Ti_3C_2 with the narrow-band gap semiconductor BiOI and CeO_2 [93]. The terpolymer photocatalyst demonstrated the highest photocatalytic antibacterial efficiency against *E. coli* and *S. aureus* (99.76% and 99.89%, respectively). The combined effects of the Schottky junction formed by CeO_2 and Ti_3C_2 and the p-n junction formed by CeO_2 and BiOI effectively promoted photogenerated electron-hole transfer, increased the production of ROS, and improved bacterial inactivation efficiency.

The unique electronic and optical properties of precious metal NPs enable plasmonic photocatalysts to induce localized surface plasmonic resonance (LSPR) effects, thereby enhancing the separation of electron-hole pairs (e^--h^+) and improving absorption properties in the visible light region. When electrons generated by metal-LSPR are in direct contact with the semiconductor, they can be effectively transferred from the precious metal to the semiconductor under irradiation. This process, driven by photocurrent under the excitation of the plasma band, depletes electrons in the plasmonic metal and facilitates redox reactions on the semiconductor surface [66,94]. Zhao et al. successfully prepared Au/g-C_3N_4/CeO_2 plasma heterojunction photocatalyst by forming three-dimensional hollow CeO_2 mesoporous nanospheres on two-dimensional Au/g-C_3N_4 nanosheets [95]. Increasing the Au loading on Au/g-C_3N_4/CeO_2 surface improved the photocatalytic performance. The LSPR effect of gold nanoparticles could expand the absorption range, improve the light absorption, and increase the electromagnetic field intensity at the metal/semiconductor interface, which helped generate more carriers, thereby enhancing the photodegradation activity. To address the issues of caking and photocorrosion in nano-silver and silver halide, which exhibit good plasmonic photocatalytic activity, Sun et al. developed an Ag@AgCl/g-C_3N_4 plasma photocatalyst through in-situ implantation and anchoring [96]. This method resulted in highly dispersed and strongly immobilized plasma heterojunctions, significantly promoting the design of highly stable plasma heterojunction nanostructured photocatalysts.

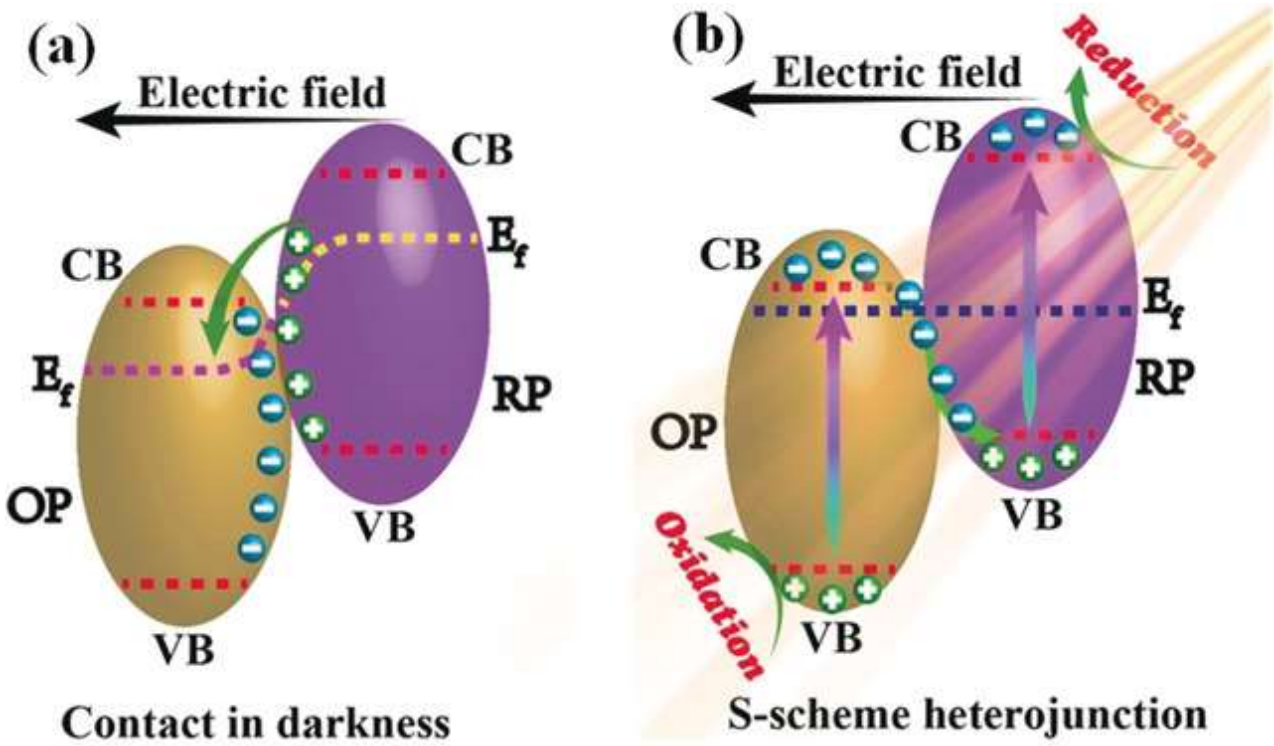

Figure 5. Diagram of (**a**) the electron transfer between RP and OP photocatalyst contacted in darkness and (**b**) photogenerated carrier transfer in the S-scheme heterojunction under illumination [90].

Electronic structure regulation is one of the most important methods for tuning photocatalytic activity, which includes element doping and oxygen vacancy engineering. Element doping involves introducing other elements into semiconductor, including both metal elements (such as Fe, Cu, Zn, Ni) and non-metal elements (such as C, O, P, S and B). Introducing doping elements into the semiconductor reduces the band gap width and alters its electronic structure, thereby expanding the absorbed radiation spectrum to higher wavelengths [97]. This process also provides more active sites for molecular adsorption and activation [86]. Iftikhar et al. combined Fe-doped CdS nanoparticles with S-doped g-C_3N_4 nanocomposites via the co-precipitation method to prepare a low-cost and non-toxic visible-driven photocatalyst [98]. A distinct heterostructure formed between Fe/CdS and S-doped g-C_3N_4, establishing a strong connection and providing numerous active sites for catalytic activity. The results indicated that element doping altered the structural composition of the original photocatalyst, with 9% Fe@CdS and 50% S-g-C_3N_4 exhibiting a synergistic effect in enhancing photocatalytic antibacterial efficacy against *S. aureus*.

Defects play a crucial role in heterogeneous catalytic reactions as they serve not only as active sites for reactant molecules but also regulate the electronic structure of the semiconductor by introducing additional energy bands between the CB and VB of the photocatalyst. Oxygen vacancies are often used as deactivation sites for catalysts and recombination centers for photogenerated carriers. By regulating oxygen vacancies, the oxidation capacity of semiconductor catalysts can be adjusted to control their activity and selectivity during photocatalytic oxidation processes [99]. Zhang et al. prepared Pt-assisted self-modified Bi_2WO_6 composites (Pt/Bi-BWO) with a high concentration of oxygen vacancies [100]. These oxygen vacancies could activate O_2 to produce ROS, thereby enhancing visible light absorption. The photocatalytic reaction rate of Pt/Bi-BWO was 2.88 times higher than that of Bi_2WO_6, as the oxygen vacancies reduced the band gap by creating isolation levels below the CB of Bi_2WO_6. Due to the high oxygen storage capacity of CeO_2, controlling its oxygen vacancies was beneficial for the adsorption and reduction of dissolved O_2.

The effectiveness of photocatalytic agents diminishes significantly under low or no light conditions, underscoring the need for further research into materials capable of maintaining antifouling performance in such environments. In response, researchers have explored several strategies to achieve antifouling effects in areas with limited or no light exposure. One approach involves developing photocatalytic materials that retain functionality under low-light or dark conditions, such as V_2O_5/$BiVO_4$ nanocomposites and WO_3, which not only exhibit excellent photocatalytic activity under visible light but also demonstrate effective contact-based antibacterial properties in the absence of light [101]. Another strategy is to combine photocatalytic materials with compounds known for their antibacterial and algal-inhibiting properties, such as indole analogues, capsaicin, and chitosan. These combinations can produce antifouling effects even in low-light environments. For instance, resins containing indole derivatives exhibit superior antifouling properties

and higher biological activity compared to pure resins [102]. The incorporation of antifouling resins with photocatalytic materials can also significantly improve the prevention of bacterial adhesion, even in low-light environments. For example, the utilization of degradable green poly-Schiff base resins has enhanced the antimicrobial efficacy of g-C_3N_4-based photocatalytic antifouling coatings, achieving antimicrobial rates of 99.31% in the dark and 99.87% under visible light conditions [103]. This dual functionality with the combination of dynamic self-renewal with photocatalytic antibacterial activity provides a promising, eco-friendly strategy for long-term antifouling in marine environments.

3.2. Combination of Resin and Inorganic Coatings with Photocatalytic Agents

Antifouling resins are a critical component of antifouling coatings, serving not only as the substrate and carrier of antifouling agents but also directly influencing the coating's performance. They control the release of antifouling agents, determining key properties such as antifouling effectiveness, environmental impact, and the coating's longevity. Physical mixing and chemical bonding are the two main approaches for photocatalytic materials binding to resins, with the latter being the more commonly employed method [104–107]. Based on their development, antifouling resins can be categorized into dissolving resins, diffused resins, self-polishing resins and low surface energy resins. Dissolved and diffused resins are now rarely used due to their short antifouling lifespan and environmental concerns. In contrast, self-polishing and low surface energy resin are extensively studied and widely applied due to their excellent properties, which, when combined with antifouling agents, yield highly effective results.

Acrylic resins, particularly zinc/copper-based acrylics, are known for excellent self-polishing properties and are frequently used in antifouling coatings. These resins have proven to be the most effective antifouling resins since the phasing out of organotin resins [102]. Sun et al. developed a composite hydrophobic coating using flower-like ZnO, water-based acrylic resin, and stearic acid [108]. The resulting coating displayed excellent hydrophobicity, photocatalytic degradation under visible light, and high durability in a 3.5 wt.% NaCl solution. Additionally, it exhibited strong resistance to water, stains, corrosion, and fouling, while also possessing self-cleaning properties. Epoxy resin, a common thermosetting resin, is recognized for its extensive crosslinking and strong physicochemical interactions with nanofillers. These properties enable it to slow the release of active ingredients from nanocomposites, providing resistance to fouling [109]. Palanivelu et al. enhanced epoxy coatings with nano-ZnO at various weight percentages, finding that 2.5 wt.% ZnO, uniformly distributed in the epoxy matrix, significantly improved the coating's barrier properties by reducing porosity. This nanocomposite coating demonstrated excellent adhesion, impact resistance, and flexibility, making it ideal for anticorrosion and antifouling applications [110].

Low surface energy resins are designed to resist the attachment of fouling organisms through their superhydrophobic or superoleophobic surfaces. Two crucial factors in the development of such coatings are the chemical structure and the appropriate surface roughness. Functional groups containing fluorine or silicon are typically added to resins to lower surface energy [111]. He et al. developed a low-surface-energy flexible antifouling coating for marine culture nets by physically blending a biogenic antibacterial component with methyl phenyl silicone resin. The coating retained the low-surface-energy properties of silicone resin, exhibiting a contact angle greater than 130° and surface energy below 1.5 mN m^{-1} [107].

Modern photocatalytic antifouling coatings are not limited to the combination of photocatalytic materials and resins but also involve composites of photocatalytic materials with inorganic coatings, which offer enhanced antifouling properties. Inorganic coatings extend light absorption into the visible spectrum and improve stability against photocorrosion. The doping of metal ions onto the surface of semiconductor nanoparticles, combined with the deposition of inorganic materials, can further enhance photocatalytic activity through interfacial charge transfer and electronic interactions between the surface layer and the host semiconductor [112]. Metal films enable more efficient light energy utilization and improve reaction kinetics by leveraging their optical and electronic properties alongside the highly active surface of photocatalysts. Additionally, metal films act as protective layers, reducing photocorrosion during the photocatalytic process and thereby enhancing the stability and longevity. Subramanian et al. employed electrophoretic deposition to coat nano-TiO_2 films with precious metal nanoparticles (Au, Pt, Ir) using tetraoctylammonium bromide (TOAB), which improved photocurrent generation, created new electron-hole recombination centers, and shifted the apparent flat band potential [113]. It has been demonstrated that surface modification of semiconductors with metal nanoparticles facilitates charge transfer processes at the interface, improving overall photocatalytic efficiency.

4. Performance Evaluation

4.1. Laboratory Evaluation of Antifouling Performance

Laboratory evaluation of antifouling performance is essential for the successful development of antifouling coatings. The antifouling performance can be investigated through the resistance assessment for biofilm, bacterial, algal and larval.

Bacteria secrete extracellular polymers, which adhere to the surface of the conditioning membrane and gradually develop into biofilms. Once mature, biofilms are difficult to remove, making it crucial to eliminate extracellular polymers early on [114]. Photocatalytic antifouling coatings generate a significant amount of ROS, which can lead to polysaccharide deterioration and affect extracellular polymeric substances and the entire bacterial cell [115]. In addition, ROS can penetrate cells through damaged membranes and cause DNA damage [116]. Therefore, the antibacterial properties of coatings can be assessed by detecting the content of biofilm and DNA. Al-For et al. found that in the presence of ZnO nanorods coating under illumination, the DNA concentration and biofilm formation were significantly reduced [117]. The inhibition effect of ZnO nanorods coating on the biofilm formation of marine bacterium *Acinetobacter* sp. AZ4C was 2.3~3.5 times greater than that of the control.

E. coli and *S. aureus*, common marine bacteria and pathogens, are primary targets for inhibition in antifouling coatings. Gao et al. successfully synthesized a new layered TiO_2/CdS composite using hydrothermal and thermal injection methods [18]. TiO_2/CdS composites exhibited excellent antibacterial ability under visible light irradiation, achieving a 99.9% killing rate of *E. coli* within 10 min. Zhang et al. prepared a new composite material (Bi_5O_7I/ZFP) consisting of Bi_5O_7I flower-like microspheres and zwitterionic fluorinated polymer (ZFP) [118]. The results demonstrated that the synergistic hydration photocatalysis enhanced its antifouling performance, with inhibition rates of 99.09% for *E. coli* and 99.66% for *S. aureus*. Other studies have also shown that photocatalytic antifouling agents exhibit strong antibacterial activity against *Salmonella*, *Bacillus subtilis*, *Staphylococcus epidermidis*, *Proteus vulgaris*, *Klebsiella pneumoniae*, *Bacillus cereus*, and *Pseudomonas aeruginosa* [119–122].

Currently, many photocatalytic coatings have demonstrated excellent inactivation abilities for harmful algae and degradation capabilities for algal toxins. In antialgal experiments, researchers frequently choose *Microcystis aeruginosa* due to its role in causing algal blooms and producing harmful microcystin toxins [123]. Fan et al. constructed a photocatalyst containing C_3N_4@UIO-66(NH_2) heterojunctions, which achieved rapid separation of photogenerated charge carriers, and significantly enhanced the inhibition of *Microcystis aeruginosa* (99.9% degradation of chlorophyll a within 180 min) [124]. Sun et al. successfully synthesized Ag_3PO_4/g-C_3N_4 photocatalyst, which achieved a 90.22% removal rate of *Microcystis aeruginosa* under visible light irradiation for 3 h [125]. ROS attack can destroy algal cell structures, leading to electrolyte leakage, protein inactivation, weakened photosynthesis, inhibited cell activity, and eventually algal cell death. Photocatalytic antifouling tests on other algae, such as *Tetraselmis* sp., *Dunaliella tertiolecta*, *Heterosigma akashiwo*, and *Karenia mikimotoi*, also showed significant density reductions [117,126–128].

Larval resistance test of the coating can also evaluate the antifouling performance. Researchers conducted various modification experiments on different photocatalysts, demonstrating good inhibition against larvae of *Bugula neritina*, *Aedes aegypti*, *Micro-Crustacean Ceriodaphnia cornuta*, and zebra fish embryos/larvae [117,120,129,130]. Al-For et al. found that ZnO nanorod coating significantly increased the mortality of *Bugula neritina* larvae under light conditions, with a mortality rate 23~25 times higher than the control, and significantly reduced larval settlement rates [117].

4.2. Methods for Evaluating Antifouling Performance

Field testing is a crucial component in predicting the antifouling performance of coatings, including evaluating the leaching rate of antifouling agents, conducting static immersion tests, performing dynamic tests, and assessing the friction resistance of the paint film.

4.2.1. Antifouling Agent Leaching Rate Test

To ensure scientific rigor and consistency in antifouling coating testing and evaluation, national and international standards provide guidance for testing methods. The Chinese national standard GB/T 6824-2008 “Determination of Copper Ion Leaching Rate in Antifouling Paints in Real Seawater” specifies methods for evaluating the leaching rate of copper ions from antifouling coatings in real seawater environments. Similarly, ISO 15181-1:2000 and ISO 15181-

2:2000 are international standards formulated by the International Organization for Standardization (ISO) for determining the leaching rate of antifouling agents. These standards cover experimental design, sample handling, and analytical methods, ensuring the comparability and consistency of test results worldwide.

Recent advancements have continuously improved and optimized laboratory testing method for determining the leaching rate of antifouling agents. For instance, Chang et al. investigated the leaching rate of copper agents under multi-factor accelerated testing (MFAT) and real seawater testing (RST) to access the antifouling performance [131]. The MFAT method could simulate long-term marine environments in a short time, providing a rapid evaluation of performance. Additionally, the study demonstrated a good correlation and acceleration effects between MFAT and RST through the use of Spearman rank correlation coefficient methods (SRCCM) and acceleration factor methods (AFM). However, laboratory accelerated tests may not fully replicate all variables present in the real marine environment, such as biological attachment and natural climate changes, which can potentially affect the accuracy of test results. The leaching efficiency of the antifouling agent determines its antifouling effect. Lagerström et al. investigated the release rates of copper and zinc from antifouling coatings under varying salinity environments and their subsequent antifouling effects [132]. Exposure tests conducted at four different salinity gradient locations along the Swedish coast revealed that copper release rates increased with salinity, while zinc release rates were more influenced by coating type and its zinc content. All tested antifouling coatings demonstrated effective prevention of hard fouling organisms, such as barnacles, across various salinity conditions. The study recommended using low-copper-content antifouling coatings in freshwater areas to reduce environmental copper emissions without compromising antifouling effectiveness. The strengths included extensive testing across salinity gradients, field exposure tests, and comparisons among multiple coatings. However, future research should focus on long-term impacts, multi-environment testing, and the biological effects of these coatings.

4.2.2. Static Test with Floating Raft Hanging Boards

The static test simulates the performance of antifouling coatings on stationary ships in ports. This test can be conducted according to the Chinese standard GB/T5370-2007, "Test Method for Antifouling Paint Samples in Shallow Sea Immersion." Similar standard methods are specified in the United States (ASTM D3623) and Japan (JIS K630-74). The antifouling performance is evaluated based on the type and extent of fouling organisms, with different scores assigned accordingly. In recent years, extensive research has been conducted in this field. Wang et al. explored modification strategies for silicone-based antifouling coatings, with static antifouling performance as a key indicator to evolute the quality of antifouling coating [133]. The study proposed strategies such as using inorganic nanofillers, surface treatments, introducing amphiphilic polymers and controllable degradable coatings, and employing multiple hydrogen bonds, metal coordination bonds, and dynamic covalent bonds. Similarly, Jiang et al. evaluated the antifouling performance of $CuO@TiO_2$ composite photocatalytic coatings in marine environments [134]. The coating effectively prevented marine fouling and maintained high photocatalytic activity under UV light. The port floating raft hanging board test, which closely simulates actual marine environments, can realistically assess the antifouling performance and stability of prepared photocatalytic coating. However, the antifouling performance of the coating is highly dependent on the UV light source, and its effectiveness may decrease under insufficient light conditions. Additionally, static tests cannot fully simulate the performance in dynamic marine environments, necessitating further validation with dynamic tests.

4.2.3. Dynamic Test

Static tests experience slow water flow, leading to the accumulation of soap layers and bacterial slime on the antifouling coating surface, which are not easily washed away by seawater. This results in the buildup of antifouling agents on the paint film. However, ships often move at high speeds, washing away these layers and accelerating the leaching of antifouling agents from the coating film. To better simulate these conditions, dynamic tests are typically employed. This method simulates ship speed by continuously rotating samples in seawater, combined with raft immersion during the marine growth season. The Chinese national standard GB/T 7789-2007, "Marine Antifouling Paint Antifouling Performance Dynamic Test Method" details the implementation steps and conditions for dynamic testing. Similarly, the U.S. standard ASTM D4939-1989 "Standard Test Method for Fouling and Hydrolysis Resistance of Antifouling Paints in Natural Seawater" provides a framework for dynamic testing. Due to annual differences in marine hydrology and biological growth, dynamic tests can only relatively measure the antifouling performance and estimate the antifouling cycle. Dynamic tests also have been employed in the laboratory evaluation of antifouling performance. Clara Arboleda-Baena et al. studied the impact of environmental factor changes on the performance of self-polishing

antifouling coatings in dynamic tests [135]. The effects of parameters such as temperature, pH, and NaCl concentration on coating performance were explored through dynamic simulation and experimental data. The coatings were more sensitive to changes in temperature and pH, with less impact from NaCl concentration changes.

4.2.4. Friction Resistance Assessment

Beyond the antifouling performance of coatings, the roughness of the paint film surface and its impact on friction resistance are also critical considerations. Antifouling coatings must have excellent antifouling performance while reducing drag to lower energy consumption. In China, the friction resistance of antifouling coatings is typically measured according to GB/T 7791-2014 "Test Method for Antifouling and Drag Reduction Performance". Similarly, the U.S. ASTM D4939-1989, "Standard Test Method for Fouling and Hydrolysis Resistance of Antifouling Paints in Natural Seawater", provides a framework for evaluating the friction resistance of antifouling paints under both dynamic and static conditions. By simulating the movement of ships in real marine environments, this standard effectively assesses the long-term performance and durability of antifouling paints. Dobretsov et al. investigated biofilm formation and friction resistance changes in different antifouling coatings in marine environments [136]. The performance of the coatings was assessed by exposing coated samples to natural marine environments and measuring their friction resistance at various time points. Significant increases in friction resistance were found after prolonged exposure, with notable differences among the coatings. Swain utilized a flow channel testing system to examine the hydrodynamic resistance changes of different antifouling coatings after biofilm accumulation [137]. The performances of the coatings after biofilm accumulation were evaluated by measuring the friction resistance on the coating surfaces. The different coatings showed varying resistance changes after biofilm accumulation, with Intersleek 700 and Hempasil X3 coatings significantly reducing biofilm attachment. Holm et al. measured the hydrodynamic resistance of antifouling coatings after biofilm accumulation using a rotating disk apparatus [138]. The friction resistance of experimental antifouling coatings was evaluated by measuring the torque on the rotating disk after biofilm accumulation. Different coatings had varying degrees of resistance increase after biofilm accumulation, with antifouling coatings exhibiting the smallest resistance change, while release coatings showed larger changes. The study highlighted that accumulated biofilm significantly increased friction resistance, and residual resistance increase persisted even after biofilm removal.

4.3. Environmental Impact and Safety of Photocatalytic Coatings

The marine environmental benefits encompass the advantages gained from utilizing and modifying the marine environment, including the enhancement of marine ecosystems, rational use of marine resources, waste reduction and treatment, and decreased energy consumption. Improvements in these areas not only elevate human quality of life but also contribute to maintaining ecological balance and promoting the sustainable development of oceans. Photocatalytic antifouling coatings are particularly promising in this regard due to their environmental friendliness and high efficiency [139]. Photocatalytic coatings effectively reduce the reliance on chemical substances, mitigating their environmental impact and lessening the overall environmental burden. Given the complexity of marine environments, these coatings demonstrate broad applicability and durability, achieving a notable balance between antibacterial efficacy, environmental protection, efficiency, low drug resistance, and broad-spectrum antibacterial properties.

To understand the long-term impacts of nanomaterials and antifouling coatings on marine ecosystems, standardized ecotoxicology testing methods and innovative experimental designs are essential. Heinlaan et al. investigated the toxicity of nano ZnO, CuO, and TiO_2 to bacteria (*Vibrio fischeri*) and crustaceans (*Daphnia magna* and *Thamnocephalus platyurus*) [140]. Utilizing a combination of traditional ecotoxicology methods and metal-specific recombinant biosensors, the study differentiated between the toxicity effects of the metal oxides and the dissolved metal ions. TiO_2 suspensions were non-toxic even at high concentrations (20 g L^{-1}), while all Zn formulations exhibited high toxicity. The toxicity of Cu compounds varied significantly, with nano CuO being more toxic than bulk CuO and $CuSO_4$. The toxicity of Zn and Cu was primarily due to the dissolved metal ions. Jarvis et al. explored the toxicity of ZnO on the copepod Acartia tonsa via phytoplankton ingestion, finding that ZnO inhibited the growth of the phytoplankton *Thalassiosira weissflogii* in a dose-dependent manner, leading to zinc accumulation in algal cells [141]. This exposure reduced the survival and reproductive rates of the copepods. Miller et al. examined the toxicity of metal nanomaterials to phytoplankton and evaluated the ability of photosynthetic efficiency to predict toxicity effects [142]. Metal nanomaterials (ZnO, Ag, CeO_2, CuO) adversely affected the population growth rate of the phytoplankton *Isochrysis galbana*, with

photosynthetic efficiency (quantum yield of photosystem II) serving as a good indicator of toxicity effects at the population level. Although high-throughput screening methods can assess numerous cellular and physiological functions, they lack predictive power for population-level effects.

Compared to traditional antifouling coatings, photocatalytic antifouling coatings offer significant environmental benefits and hold promise for widespread application due to their high environmental performance. However, to avoid repeating past mistakes with substances like TBT, it is crucial to develop more efficient photocatalytic coatings and conduct comprehensive environmental risk assessments. The economic costs, application complexities, durability, and resource utilization of each improvement option must be weighed against their potential benefits.

5. Conclusions and Perspectives

Since the ban on tributyltin-based antifouling coatings in 2003, the search for environmentally friendly alternatives has intensified. Developing and designing new photocatalytic antifouling agents that respond to visible light and are environmentally friendly is of great practical significance for effectively utilizing solar energy and minimizing the harm of antifouling materials to the environment and human health. Photocatalytic coating, activated by visible light, generate strong oxidizing substances that effectively degrade environmental organic matter and exhibit excellent bactericidal performance. This technology significantly delays marine pollution and fouling. Commercial marine coatings based on photocatalysts have the following features: (1) Light energy from the sun or artificial sources is converted into chemical energy, producing water vapor and multiple ROS on the coating surface to kill fouling organisms; (2) Light excitation induces several reactions on the coating surface; (3) Light stimulation creates a self-cleaning effect on the coating surface; (4) The coatings are transparent and suitable for various surfaces.

Substantial progress has been made in evaluating the antifouling properties of photocatalytic coatings. Improved test schemes, new materials, and advanced characterization techniques have enhanced their antifouling properties and reduced their environmental impact. However, coatings degrade over time due to aging and wear, posing significant economic and ecological concerns. While theoretically promising for environmentally friendly marine antifouling, photocatalytic coatings are highly dependent on light. Their performance diminishes significantly under low or no light conditions, highlighting the need for further research into materials that maintain antifouling performance in weak or dark light. It is necessary to study the application prospect of photocatalytic ship antifouling technology, especially to develop dual-function photoactivated antifouling materials that can work in the absence of light.

Photocatalytic antifouling materials have applications beyond ship antifouling, where they help reduce navigation resistance and fuel consumption caused by biofouling. These materials are also used in seawater desalination equipment to prevent microbial pollution and biofilm formation. Furthermore, in marine sensor protection, photocatalytic materials prevent the attachment of marine organisms, ensuring the accuracy and stability of sensor readings. In the development of marine resources, such as offshore oil platforms and subsea pipelines, photocatalytic antifouling technology plays a crucial role in preventing the accumulation of marine organisms, reducing maintenance costs, and mitigating the risk of equipment damage. However, the efficiency of photocatalysis technology is influenced by various factors such as light intensity, seawater salinity, temperature, pH, and catalyst type, leading to unstable treatment efficiency and occasionally poor treatment outcomes. Practical applications of photocatalytic materials still face significant challenges in terms of catalyst support, activity preservation, and long-term antifouling. Further research and exploration are required to address these challenges. Additionally, the lack of large-scale industrialization and high practical performance necessitates future research to focus on developing and utilizing innovative materials and methods to improve the durability, effectiveness, and sustainability of antifouling coatings. Strengthening the recovery and reuse of catalyst technology is also crucial for reducing treatment costs.

Acknowledgments

W. Xiong is grateful for support from the Key Laboratory of Industrial Ecology and Environmental Engineering (Ministry of Education) and Ability R&D Energy Research Centre, School of Energy and Environment, City University of Hong Kong.

Author Contributions

Writing—Original Draft Preparation, W.B., H.L.; Writing—Review & Editing, W.X.; Supervision, M.K.H.L.; Funding Acquisition, M.K.H.L.

Ethics Statement

Not applicable.

Informed Consent Statement

Not applicable.

Funding

This research was funded by Research Grants Council of the Hong Kong (Project No. CityU 11206520) and Innovation and Technology Fund (PRP/002/21FX).

Declaration of Competing Interest

The authors declare that they have no known competing financial interests or personal relationships that could have appeared to influence the work reported in this paper.

References

1. Satheesh S, Ba-akdah MA, Al-Sofyani AA. Natural antifouling compound production by microbes associated with marine macroorganisms—A review. *Electron. J. Biotechn.* **2016**, *21*, 26–35.
2. Xie C, Guo H, Zhao W, Zhang L. Environmentally Friendly Marine Antifouling Coating Based on a Synergistic Strategy. *Langmuir* **2020**, *36*, 2396–2402.
3. Li S, Feng K, Li J, Li Y, Li Z, Yu L, et al. Marine antifouling strategies: Emerging opportunities for seawater resource utilization. *Chem. Eng. J.* **2024**, *486*, 149859.
4. Miralles L, Ardura A, Arias A, Borrell YJ, Clusa L, Dopico E, et al. Barcodes of marine invertebrates from north Iberian ports: Native diversity and resistance to biological invasions. *Mar. Pollut. Bull.* **2016**, *112*, 183–188.
5. Hellio DYC. Advances in Marine Antifouling Coatings and Technologies, 1st ed.; Woodhead Publishing: San Diego, CA, USA, 2009.
6. Magin CM, Cooper SP, Brennan AB. Non-toxic antifouling strategies. *Mater. Today* **2010**, *13*, 36–44.
7. Selim MS, Shenashen MA, El-Safty SA, Higazy SA, Selim MM, Isago H, et al. Recent progress in marine foul-release polymeric nanocomposite coatings. *Prog. Mater Sci.* **2017**, *87*, 1–32.
8. Lee W, Ahn CH, Hong S, Kim S, Lee S, Baek Y, et al. Evaluation of surface properties of reverse osmosis membranes on the initial biofouling stages under no filtration condition. *J. Membr. Sci.* **2010**, *351*, 112–122.
9. Almeida E, Diamantino TC, de Sousa O. Marine paints: The particular case of antifouling paints. *Prog. Org. Coat.* **2007**, *59*, 2–20.
10. Yang WJ, Neoh K-G, Kang E-T, Teo SL-M, Rittschof D. Polymer brush coatings for combating marine biofouling. *Prog. Polym. Sci.* **2014**, *39*, 1017–1042.
11. Lejars M, Margaillan A, Bressy C. Fouling Release Coatings: A Nontoxic Alternative to Biocidal Antifouling Coatings. *Chem. Rev.* **2012**, *112*, 4347–4390.
12. Liu D, Shu H, Zhou J, Bai X, Cao P. Research Progress on New Environmentally Friendly Antifouling Coatings in Marine Settings: A Review. *Biomimetics* **2023**, *8*, 200.
13. Callow JA, Callow ME. Trends in the development of environmentally friendly fouling-resistant marine coatings. *Nat. Commun.* **2011**, *2*, 244.
14. Trávníčková E, Pijáková B, Marešová D, Bláha L. Antifouling performance of photocatalytic superhydrophobic coatings against Klebsormidium alga. *J. Environ. Chem. Eng.* **2020**, *8*, 104153.
15. Hu H, Chen M, Cao M. TiO_2 antifouling coating based on epoxy-modified tung oil waterborne resin. *Polym. Polym. Compos.* **2021**, *29* (9_suppl), S521–S529.
16. Mahy JG, Cerfontaine V, Poelman D, Devred F, Gaigneaux EM, Heinrichs B, et al. Highly Efficient Low-Temperature N-Doped TiO_2 Catalysts for Visible Light Photocatalytic Applications. *Materials* **2018**, *11*, 584.
17. Bai H, Liu Z, Liu L, Sun DD. Large-scale production of hierarchical TiO_2 nanorod spheres for photocatalytic elimination of contaminants and killing bacteria. *Chemistry* **2013**, *19*, 3061–3070.
18. Gao P, Liu J, Zhang T, Sun DD, Ng W. Hierarchical TiO_2/CdS "spindle-like" composite with high photodegradation and antibacterial capability under visible light irradiation. *J. Hazard. Mater.* **2012**, *229–230*, 209–216.
19. Wang X, Li S, Chen P, Li F, Hu X, Hua T. Photocatalytic and antifouling properties of TiO_2-based photocatalytic membranes. *Mater. Today Chem.* **2022**, *23*, 100650.
20. Li L, Hong H, Cao J, Yang Y. Progress in Marine Antifouling Coatings: Current Status and Prospects. *Coatings* **2023**, *13*, 1893.

21. Amara I, Miled W, Slama RB, Ladhari N. Antifouling processes and toxicity effects of antifouling paints on marine environment. A review. *Environ. Toxicol. Pharmacol.* **2018**, *57*, 115–130.
22. Liu J, Li Q, Meng F, Zhang T, Gao F, Zhan X, et al. Recent progress in fabrications, mechanisms and developments of photoresponsive marine antifouling coatings. *Prog. Org. Coat.* **2024**, *186*, 108070.
23. Furdek M, Mikac N, Bueno M, Tessier E, Cavalheiro J, Monperrus M. Organotin persistence in contaminated marine sediments and porewaters: In situ degradation study using species-specific stable isotopic tracers. *J. Hazard. Mater.* **2016**, *307*, 263–273.
24. Mikac N, Turk MF, Petrović D, Bigović M, Krivokapić S. First assessment of butyltins (BuTs) contamination of the Montenegrin coast (Southeast Adriatic): Tributyltin (TBT) poses a threat to the marine ecosystem. *Mar. Pollut. Bull.* **2022**, *185*, 114270.
25. Beyer J, Song Y, Tollefsen KE, Berge JA, Tveiten L, Helland A, et al. The ecotoxicology of marine tributyltin (TBT) hotspots: A review. *Mar. Environ. Res.* **2022**, *179*, 105689.
26. Alzieu C. Environmental impact of TBT: The French experience. *Sci. Total Environ.* **2000**, *258*, 99–102.
27. Gipperth L. The legal design of the international and European Union ban on tributyltin antifouling paint: Direct and indirect effects. *J. Environ. Manag.* **2009**, *90*, S86–S95.
28. Oliveira ICCS, Marinsek GP, Correia LVB, da Silva RCB, Castro IB, Mari RB. Tributyltin (TBT) toxicity: Effects on enteric neuronal plasticity and intestinal barrier of rats' duodenum. *Auton. Neurosci.* **2024**, *253*, 103176.
29. Dafforn KA, Lewis JA, Johnston EL. Antifouling strategies: History and regulation, ecological impacts and mitigation. *Mar. Pollut. Bull.* **2011**, *62*, 453–465.
30. Briant N, Freydier R, Araújo DF, Delpoux S, Elbaz-Poulichet F. Cu isotope records of Cu-based antifouling paints in sediment core profiles from the largest European Marina, The Port Camargue. *Sci. Total Environ.* **2022**, *849*, 157885.
31. Gu Y, Yu L, Mou J, Wu D, Xu M, Zhou P, et al. Research Strategies to Develop Environmentally Friendly Marine Antifouling Coatings. *Mar. Drugs* **2020**, *18*, 371.
32. Thomas KV. The environmental fate and behaviour of antifouling paint booster biocides: A review. *Biofouling* **2001**, *17*, 73–86.
33. Konstantinou IK, Albanis TA. Worldwide occurrence and effects of antifouling paint booster biocides in the aquatic environment: A review. *Environ. Int.* **2004**, *30*, 235–248.
34. Gaw SL, Sarkar S, Nir S, Schnell Y, Mandler D, Xu ZJ, et al. Electrochemical Approach for Effective Antifouling and Antimicrobial Surfaces. *ACS Appl. Mater. Interfaces* **2017**, *9*, 26503–26509.
35. Ackermann S, Steimecke M, Morig C, Spohn U, Bron M. A complementary Raman and SECM study on electrically conductive coatings based on graphite sol-gel composite electrodes for the electrochemical antifouling. *J. Electroanal. Chem.* **2017**, *795*, 68–74.
36. Jia M-Y, Zhang Z-M, Yu L-M, Wang J, Zheng T-T. The feasibility and application of PPy in cathodic polarization antifouling. *Colloids Surf. B* **2018**, *164*, 247–254.
37. Wake H, Takimoto T, Takayanagi H, Ozawa K, Kadoi H, Mukai S, et al. Construction of an Electrochemical Antibiofouling System for Plate Heat Exchangers. *J. Chem. Eng. Jpn.* **2010**, *43*, 608–611.
38. Pérez-Roa RE, Anderson MA, Rittschof D, Hunt CG, Noguera DR. Involvement of reactive oxygen species in the electrochemical inhibition of barnacle (Amphibalanus amphitrite) settlement. *Biofouling* **2009**, *25*, 563–571.
39. Jin H, Tian L, Bing W, Zhao J, Ren L. Bioinspired marine antifouling coatings: Status, prospects, and future. *Prog. Mater Sci.* **2022**, *124*, 100889.
40. Levert A, Foulon V, Fauchon M, Tapissier-Bontemps N, Banaigs B, Hellio C. Antifouling Activity of Meroterpenes Isolated from the Ascidian *Aplidium aff. densum*. *Mar. Biotechnol.* **2020**, *23*, 51–61.
41. Darya M, Abdolrasouli MH, Yousefzadi M, Sajjadi MM, Sourinejad I, Zarei M. Antifouling coating based on biopolymers (PCL/PLA) and bioactive extract from the sea cucumber *Stichopus herrmanni*. *AMB Express* **2022**, *12*, 24.
42. Arzt E, Quan H, McMeeking RM, Hensel R. Functional surface microstructures inspired by nature—From adhesion and wetting principles to sustainable new devices. *Prog. Mater Sci.* **2021**, *120*, 100823.
43. Guan Y, Chen R, Sun G, Liu Q, Liu J, Yu J, et al. The mussel-inspired micro-nano structure for antifouling:A flowering tree. *J. Colloid Interface Sci.* **2021**, *603*, 307–318.
44. Xue L, Lu X, Wei H, Long P, Xu J, Zheng Y. Bio-inspired self-cleaning PAAS hydrogel released coating for marine antifouling. *J. Colloid Interface Sci.* **2014**, *421*, 178–183.
45. Yang J, Xue B, Zhou Y, Qin M, Wang W, Cao Y. Spray-Painted Hydrogel Coating for Marine Antifouling. *Adv. Mater. Technol.* **2021**, *6*, 2000911.
46. Peppou-Chapman S, Hong JK, Waterhouse A, Neto C. Life and death of liquid-infused surfaces: A review on the choice, analysis and fate of the infused liquid layer. *Chem. Soc. Rev.* **2020**, *49*, 3688–3715.
47. Tong Z, Song L, Chen S, Hu J, Hou Y, Liu Q, et al. Hagfish-inspired Smart SLIPS Marine Antifouling Coating Based on Supramolecular: Lubrication Modes Responsively Switching and Self-healing Properties. *Adv. Funct. Mater.* **2022**, *32*, 2201290.

48. Bode-Aluko CA, Pereao O, Kyaw HH, Al-Naamani L, Al-Abri MZ, Myint MTZ, et al. Photocatalytic and antifouling properties of electrospun TiO_2 polyacrylonitrile composite nanofibers under visible light. *Mater. Sci. Eng. B* **2021**, *264*, 114913.
49. Mesquita MQ, Dias CJ, Neves MG, Almeida A, Faustino MAF. Revisiting Current Photoactive Materials for Antimicrobial Photodynamic Therapy. *Molecules* **2018**, *23*, 2424.
50. Tokode O, Prabhu R, Lawton LA, Robertson PKJ. Controlled periodic illumination in semiconductor photocatalysis. *J. Photochem. Photobiol. A* **2016**, *319–320*, 96–106.
51. Tong H, Ouyang S, Bi Y, Umezawa N, Oshikiri M, Ye J. Nano-photocatalytic Materials: Possibilities and Challenges. *Adv. Mater.* **2012**, *24*, 229–251.
52. Foster HA, Ditta IB, Varghese S, Steele A. Photocatalytic disinfection using titanium dioxide: Spectrum and mechanism of antimicrobial activity. *Appl. Microbiol. Biotechnol.* **2011**, *90*, 1847–1868.
53. Nosaka Y, Nosaka AY. Generation and Detection of Reactive Oxygen Species in Photocatalysis. *Chem. Rev.* **2017**, *117*, 11302–11336.
54. Teng Z, Yang N, Lv H, Wang S, Hu M, Wang C, et al. Edge-Functionalized g-C_3N_4 Nanosheets as a Highly Efficient Metal-free Photocatalyst for Safe Drinking Water. *Chem* **2019**, *5*, 664–680.
55. Zhang X, Zhang S, Mathivanan K, Zhang R, Zhang J, Jiang Q, et al. Research progress and prospects in antifouling performance of photocatalytic sterilization: A review. *J. Mater. Sci. Technol.* **2025**, *208*, 189–201.
56. Liang Y, Xu W, Fang J, Liu Z, Chen D, Pan T, et al. Highly dispersed bismuth oxide quantum dots/graphite carbon nitride nanosheets heterojunctions for visible light photocatalytic redox degradation of environmental pollutants. *Appl. Catal. B-Environ.* **2021**, *295*, 120279.
57. Liu M, Li S, Wang H, Jiang R, Zhou X. Research progress of environmentally friendly marine antifouling coatings. *Polym. Chem.* **2021**, *12*, 3702–3720.
58. Li S, Hu J. Photolytic and photocatalytic degradation of tetracycline: Effect of humic acid on degradation kinetics and mechanisms. *J. Hazard. Mater.* **2016**, *318*, 134–144.
59. Carrier AJ, Carve M, Shimeta J, Walker TR, Zhang X, Oakes KD, et al. Transitioning towards environmentally benign marine antifouling coatings. *Front. Mar. Sci.* **2023**, *10*, 1175270.
60. Sun X, Wang C, Su D, Wang G, Zhong Y. Application of Photocatalytic Materials in Sensors. *Adv. Mater. Technol.* **2020**, *5*, 1900993.
61. Allen NS, Edge M, Sandoval G, Verran J, Stratton J, Maltby J. Photocatalytic Coatings for Environmental Applications. *Photochem. Photobiol.* **2005**, *81*, 279–290.
62. Miyagi T, Kamei M, Mitsuhashi T, Ishigaki T, Yamazaki A. Charge separation at the rutile/anatase interface: A dominant factor of photocatalytic activity. *Chem. Phys. Lett.* **2004**, *390*, 399–402.
63. Valenzuela L, Iglesias A, Faraldos M, Bahamonde A, Rosal R. Antimicrobial surfaces with self-cleaning properties functionalized by photocatalytic ZnO electrosprayed coatings. *J. Hazard. Mater.* **2019**, *369*, 665–673.
64. Choudhary S, Sahu K, Bisht A, Singhal R, Mohapatra S. Template-free and surfactant-free synthesis of CeO_2 nanodiscs with enhanced photocatalytic activity. *Appl. Surf. Sci.* **2020**, *503*, 144102.
65. Lin H, Tang X, Wang J, Zeng Q, Chen H, Ren W, et al. Enhanced visible-light photocatalysis of clofibric acid using graphitic carbon nitride modified by cerium oxide nanoparticles. *J. Hazard. Mater.* **2021**, *405*, 124204.
66. Fauzi AA, Jalil AA, Hassan NS, Aziz FFA, Azami MS, Hussain I, et al. A critical review on relationship of CeO_2-based photocatalyst towards mechanistic degradation of organic pollutant. *Chemosphere* **2022**, *286*, 131651.
67. Moniz SJA, Shevlin SA, Martin DJ, Guo Z-X, Tang J. Visible-light driven heterojunction photocatalysts for water splitting—A critical review. *Energy Environ. Sci.* **2015**, *8*, 731–759.
68. Wang X, Deng M, Zhao Z, Zhang Q, Wang Y. Synthesis of super-hydrophobic CuO/ZnO layered composite nano-photocatalyst. *Mater. Chem. Phys.* **2022**, *276*, 125305.
69. Barman D, Borah J, Deb S, Sarma BK. Design strategy for CuO-ZnO S-scheme heterojunction photocatalysts in the presence of plasmonic Ag and insights into photoexcited carrier generation and interfacial transfer in diverse structural configurations of the heterostructure system. *Colloids Surf. A* **2023**, *663*, 131077.
70. Sharma P, Pant S, Dave V, Tak K, Sadhu V, Reddy KR. Green synthesis and characterization of copper nanoparticles by Tinospora cardifolia to produce nature-friendly copper nano-coated fabric and their antimicrobial evaluation. *J. Microbiol. Methods* **2019**, *160*, 107–116.
71. Liang Y-C, Chung C-C, Lin T-Y, Cheng Y-R. Synthesis and microstructure-dependent photoactivated properties of three-dimensional cadmium sulfide crystals. *J. Alloys Compd.* **2016**, *688*, 769–775.
72. Ai Z, Huang M, Shi D, Yang M, Hu H, Zhang B, et al. Phase engineering of CdS optimized by BP with p-n junction: Establishing spatial-gradient charges transmission mode toward efficient photocatalytic water reduction. *Appl. Catal. B-Environ.* **2022**, *315*, 121577.
73. Jie L, Gao X, Cao X, Wu S, Long X, Ma Q, et al. A review of CdS photocatalytic nanomaterials: Morphology, synthesis methods, and applications. *Mater. Sci. Semicond. Process.* **2024**, *176*, 108288.

74. Wang L, Liu Z, Han J, Li R, Huang M. Stepwise Synthesis of Au@CdS-CdS Nanoflowers and Their Enhanced Photocatalytic Properties. *Nanoscale Res. Lett.* **2019**, *14*, 148.
75. Ong WJ, Tan LL, Ng YH, Yong ST, Chai SP. Graphitic Carbon Nitride (g-C_3N_4)-Based Photocatalysts for Artificial Photosynthesis and Environmental Remediation: Are We a Step Closer To Achieving Sustainability? *Chem. Rev.* **2016**, *116*, 7159–7329.
76. Feng Y, Liao C, Kong L, Wu D, Liu Y, Lee P-H, et al. Facile synthesis of highly reactive and stable Fe-doped g-C_3N_4 composites for peroxymonosulfate activation: A novel nonradical oxidation process. *J. Hazard. Mater.* **2018**, *354*, 63–71.
77. Liu H, Ma S, Shao L, Liu H, Gao Q, Li B, et al. Defective engineering in graphitic carbon nitride nanosheet for efficient photocatalytic pathogenic bacteria disinfection. *Appl. Catal. B-Environ.* **2020**, *261*, 118201.
78. Chen Q, Cheng X, Long H, Rao Y. A short review on recent progress of Bi/semiconductor photocatalysts: The role of Bi metal. *Chin. Chem. Lett.* **2020**, *31*, 2583–2590.
79. Song Y, Long A, Ge X, Bao Z, Meng M, Hu S, et al. Construction of floatable flower-like plasmonic Bi/BiOCl-loaded hollow kapok fiber photocatalyst for efficient degradation of RhB and antibiotics. *Chemosphere* **2023**, *343*, 140240.
80. Wu D, Wang B, Wang W, An TC, Li GY, Ng TW, et al. Visible-light-driven BiOBr nanosheets for highly facet-dependent photocatalytic inactivation of *Escherichia coli*. *J. Mater. Chem. A* **2015**, *3*, 15148–15155.
81. Zhang Y, Ju P, Wang N, Nicholas CCH, Dou K, Zhai X, et al. Highly efficient photocatalytic antifouling activity of core-shell structural encapsulation Bi_2MoO_6 with visible-light responsive ZIF-67. *Appl. Surf. Sci.* **2024**, *653*, 159353.
82. Boppella R, Yang W, Tan J, Kwon H-C, Park J, Moon J. Black phosphorus supported Ni_2P co-catalyst on graphitic carbon nitride enabling simultaneous boosting charge separation and surface reaction. *Appl. Catal. B-Environ.* **2019**, *242*, 422–430.
83. Zhang Z, He D, Zhou Y, Bai E, Qu J, Zhang Y. Fabrication of black phosphorus/CdS heterostructure with enhancement photocatalytic degradation activity for tetrabromobisphenol A and toxicity prediction of intermediates. *Environ. Res.* **2024**, *256*, 119060.
84. Liang M, Zhang M, Yu S, Wu Q, Ma K, Chen Y, et al. Silver-Laden Black Phosphorus Nanosheets for an Efficient In Vivo Antimicrobial Application. *Small* **2020**, *16*, 1905938.
85. Xiao M, Wang Z, Lyu M, Luo B, Wang S, Liu G, et al. Hollow Nanostructures for Photocatalysis: Advantages and Challenges. *Adv. Mater.* **2019**, *31*, e1801369.
86. Yang S, Zhang F, Shang Y, Luo L, Liu Z. Highly efficient photocatalytic degradation of refractory organic pollutants onto designed boron nitride: Morphology control and oxygen doping. *J. Clean. Prod.* **2023**, *429*, 139532.
87. Xiang Z, Wang Y, Ju P, Zhang D. Controlled Synthesis and Photocatalytic Antifouling Properties of $BiVO_4$ with Tunable Morphologies. *J. Electron. Mater.* **2017**, *46*, 758–765.
88. He H, Luo Z, Yu C. Multifunctional $ZnWO_4$ nanoparticles for photocatalytic removal of pollutants and disinfection of bacteria. *J. Photoch. Photobio. A* **2020**, *401*, 112735.
89. He H, Luo Z, Yu C. Embellish zinc tungstate nanorods with silver chloride nanoparticles for enhanced photocatalytic, antibacterial and antifouling performance. *Colloid Surf. Physicochem. Eng. Asp.* **2021**, *613*, 126099.
90. Xia P, Cao S, Zhu B, Liu M, Shi M, Yu J, et al. Designing a 0D/2D S-Scheme Heterojunction over Polymeric Carbon Nitride for Visible-Light Photocatalytic Inactivation of Bacteria. *Angew. Chem. Int. Ed.* **2020**, *59*, 5218–5225.
91. Thongjamroon S, Wootthikanokkhan J, Poolthong N. Photocatalytic Performances and Antifouling Efficacies of Alternative Marine Coatings Derived from Polymer/Metal Oxides (WO_3@TiO_2)-Based Composites. *Catalysts* **2023**, *13*, 649.
92. Lv Y, Zheng Y, Zhu H, Wu Y. Designing a dual-functional material with barrier anti-corrosion and photocatalytic antifouling properties using g-C_3N_4 nanosheet with ZnO nanoring. *J. Mater. Sci. Technol.* **2022**, *106*, 56–69.
93. Mao Z, Hao W, Wang W, Ma F, Ma C, Chen S. BiOI@CeO_2@Ti_3C_2 MXene composite S-scheme photocatalyst with excellent bacteriostatic properties. *J. Colloid Interface Sci.* **2023**, *633*, 836–850.
94. Amoli-Diva M, Anvari A, Sadighi-Bonabi R. Synthesis of magneto-plasmonic Au-Ag NPs-decorated TiO_2-modified Fe_3O_4 nanocomposite with enhanced laser/solar-driven photocatalytic activity for degradation of dye pollutant in textile wastewater. *Ceram. Int.* **2019**, *45*, 17837–17846.
95. Zhao W, Dong Q, Sun C, Xia D, Huang H, Yang G, et al. A novel Au/g-C_3N_4 nanosheets/CeO_2 hollow nanospheres plasmonic heterojunction photocatalysts for the photocatalytic reduction of hexavalentchromium and oxidation of oxytetracycline hydrochloride. *Chem. Eng. J.* **2021**, *409*, 128185.
96. Sun D, Zhang Y, Liu Y, Wang Z, Chen X, Meng Z, et al. In-situ homodispersely immobilization of Ag@AgCl on chloridized g-C_3N_4 nanosheets as an ultrastable plasmonic photocatalyst. *Chem. Eng. J.* **2020**, *384*, 123259.
97. Długosz O, Wąsowicz N, Szostak K, Banach M. Photocatalytic properties of coating materials enriched with bentonite/ZnO/CuO nanocomposite. *Mater. Chem. Phys.* **2021**, *260*, 124150.
98. Iftikhar A, Javed M, Mansoor S, Mahmood S, Iqbal S, Aslam M, et al. Fe-doped CdS with sulfonated g-C_3N_4 in a heterojunction designed for improved biomedical and photocatalytic potentials. *Inorg. Chem. Commun.* **2024**, *162*, 112205.
99. Bui HT, Weon S, Bae JW, Kim E-J, Kim B, Ahn Y-Y, et al. Oxygen vacancy engineering of cerium oxide for the selective photocatalytic oxidation of aromatic pollutants. *J. Hazard. Mater.* **2021**, *404*, 123976.

100. Zhang S, Pu W, Chen A, Xu Y, Wang Y, Yang C, et al. Oxygen vacancies enhanced photocatalytic activity towards VOCs oxidation over Pt deposited Bi_2WO_6 under visible light. *J. Hazard. Mater.* **2020**, *384*, 121478.
101. Wang Y, Long Y, Zhang D. Novel bifunctional V_2O_5/$BiVO_4$ nanocomposite materials with enhanced antibacterial activity. *J. Taiwan Inst. Chem. Eng.* **2016**, *68*, 387–395.
102. Ni C, Feng K, Li X, Zhao H, Yu L. Study on the preparation and properties of new environmentally friendly antifouling acrylic metal salt resins containing indole derivative group. *Prog. Org. Coat.* **2020**, *148*, 105824.
103. Wu S, Yan M, Wu Y, Wu Y, Lan X, Cheng J, et al. Designing a photocatalytic and self-renewed g-C_3N_4 nanosheet/poly-Schiff base composite coating towards long-term biofouling resistance. *Mater. Horiz.* **2024**, *11*, 4438–4453.
104. Sodagar A, Khalil S, Kassaee M, Shahroudi A, Pourakbari B, Bahador A. Antimicrobial properties of poly (methyl methacrylate) acrylic resins incorporated with silicon dioxide and titanium dioxide nanoparticles on cariogenic bacteria. *J. Orthod. Sci.* **2016**, *5*, 7–13.
105. Du B, Chen F, Luo R, Zhou S, Wu Z. Synthesis and Characterization of Nano-TiO_2/SiO_2-Acrylic Composite Resin. *Adv. Mater. Sci. Eng.* **2019**, *2019*, 1–7.
106. Vu TV, Nguyen TV, Tabish M, Ibrahim S, Hoang THT, Gupta RK, et al. Water-Borne ZnO/Acrylic Nanocoating: Fabrication, Characterization, and Properties. *Polymers* **2021**, *13*, 717.
107. He G, Li H, Zhao Z, Liu Q, Yu J, Ji Z, et al. Antifouling coatings based on the synergistic action of biogenic antimicrobial agents and low surface energy silicone resins and their application to marine aquaculture nets. *Prog. Org. Coat.* **2024**, *195*, 108656.
108. Sun C, Dai J, Zhang H, Li S, Hu R. Construction of a Hydrophobic Composite Coating with Waterborne Acrylic Resin and Flower-Shaped ZnO. *Surf. Rev. Lett.* **2021**, *28*, 2150045.
109. Vijayan PP, Formela K, Saeb MR, Chithra PG, Thomas S. Integration of antifouling properties into epoxy coatings: A review. *J. Coat. Technol. Res.* **2022**, *19*, 269–284.
110. Palanivelu S, Dhanapal D, Srinivasan AK. Studies on Silicon Containing Nano-hybrid Epoxy Coatings for the Protection of Corrosion and Bio-Fouling on Mild Steel. *Silicon* **2017**, *9*, 447–458.
111. Zhu C, Yang H, Liang H, Wang Z, Dong J, Xiong L, et al. A Novel Synthetic UV-Curable Fluorinated Siloxane Resin for Low Surface Energy Coating. *Polymers* **2018**, *10*, 979.
112. Soltani N, Saion E, Yunus WMM, Erfani M, Navasery M, Bahmanrokh G, et al. Enhancement of visible light photocatalytic activity of ZnS and CdS nanoparticles based on organic and inorganic coating. *Appl. Surf. Sci.* **2014**, *290*, 440–447.
113. Subramanian V, Wolf E, Kamat PV. Semiconductor-Metal Composite Nanostructures. To What Extent Do Metal Nanoparticles Improve the Photocatalytic Activity of TiO_2 Films? *J. Phys. Chem. B* **2001**, *105*, 11439–11446.
114. Zang X, Ni Y, Wang Q, Cheng Y, Huang J, Cao X, et al. Non-toxic evolution: Advances in multifunctional antifouling coatings. *Mater. Today* **2024**, *75*, 210–243.
115. Gladis F, Eggert A, Karsten U, Schumann R. Prevention of biofilm growth on man-made surfaces: Evaluation of antialgal activity of two biocides and photocatalytic nanoparticles. *Biofouling* **2010**, *26*, 89–101.
116. Baruah S, Jaisai M, Imani R, Nazhad MM, Dutta J. Photocatalytic paper using zinc oxide nanorods. *Sci. Technol. Adv. Mater.* **2010**, *11*, 055002.
117. Al-Fori M, Dobretsov S, Myint MTZ, Dutta J. Antifouling properties of zinc oxide nanorod coatings. *Biofouling* **2014**, *30*, 871–882.
118. Zhang L, Sha J, Chen R, Liu Q, Liu J, Yu J, et al. Three-dimensional flower-like shaped Bi_5O_7I particles incorporation zwitterionic fluorinated polymers with synergistic hydration-photocatalytic for enhanced marine antifouling performance. *J. Hazard. Mater.* **2020**, *389*, 121854.
119. Shaban M, Rabia M, Fathallah W, El-Mawgoud NA, Mahmoud A, Hussien H, et al. Preparation and Characterization of Polyaniline and Ag/Polyaniline Composite Nanoporous Particles and Their Antimicrobial Activities. *J. Polym. Environ.* **2018**, *26*, 434–442.
120. Udayabhanu J, Kannan V, Tiwari M, Natesan G, Giovanni B, Perumal V. Nanotitania crystals induced efficient photocatalytic color degradation, antimicrobial and larvicidal activity. *J. Photochem. Photobiol. B* **2018**, *178*, 496–504.
121. Zewde D, Geremew B. Biosynthesis of ZnO nanoparticles using *Hagenia abyssinica* leaf extracts their photocatalytic and antibacterial activities. *Environ. Pollut. Bioavailab.* **2022**, *34*, 224–235.
122. Antonette LC, Shanthi J. Degradation of methylene blue using Methyltrimethoxysilane doped ZnO nanoparticles and inactivation of gram (+ve) and (-ve) bacteria. *Results Chem.* **2023**, *6*, 100998.
123. Hu L, Wang R, Wang M, Xu Y, Wang C, Liu Y, et al. Research progress of photocatalysis for algae killing and inhibition: A review. *Environ. Sci. Pollut. Res.* **2022**, *29*, 47902–47914.
124. Fan G, Zhan J, Luo J, Lin J, Qu F, Du B, et al. Fabrication of heterostructured Ag/AgCl@g-C_3N_4@UIO-66(NH_2) nanocomposite for efficient photocatalytic inactivation of *Microcystis aeruginosa* under visible light. *J. Hazard. Mater.* **2021**, *404*, 124062.
125. Sun S, Tang Q, Zhou L, Gao Y, Zhang W, Liu W, et al. Exploring the photocatalytic inactivation mechanism of *Microcystis aeruginosa* under visible light using Ag_3PO_4/g-C_3N_4. *Environ. Sci. Pollut. Res.* **2022**, *29*, 29993–30003.

126. Thakkar M, Mitra S, Wei L. Effect on Growth, Photosynthesis, and Oxidative Stress of Single Walled Carbon Nanotubes Exposure to Marine Alga *Dunaliella tertiolecta*. *J. Nanomater.* **2016**, *2016*, 8380491.
127. Pikula KS, Zakharenko AM, Chaika VV, Vedyagin AA, Orlova TY, Mishakov IV, et al. Effects of carbon and silicon nanotubes and carbon nanofibers on marine microalgae *Heterosigma akashiwo*. *Environ. Res.* **2018**, *166*, 473–480.
128. Wang W, Liao P, Li G, Chen H, Cen J, Lu S, et al. Photocatalytic inactivation and destruction of harmful microalgae Karenia mikimotoi under visible-light irradiation: Insights into physiological response and toxicity assessment. *Environ. Res.* **2021**, *198*, 111295.
129. Rekha R, Divya M, Govindarajan M, Alharbi NS, Kadaikunnan S, Khaled JM, et al. Synthesis and characterization of crustin capped titanium dioxide nanoparticles: Photocatalytic, antibacterial, antifungal and insecticidal activities. *J. Photochem. Photobiol. B* **2019**, *199*, 111620.
130. Deenathayalan U, Nandita R, Kavithaa K, Kavitha VS, Govindasamy C, Al-Numair KS, et al. Evaluation of Developmental Toxicity and Oxidative Stress Caused by Zinc Oxide Nanoparticles in Zebra Fish Embryos/ Larvae. *Appl. Biochem. Biotechnol.* **2023**, *196*, 4954–4973.
131. Chang M, Jia J, Huang C, Zhang S, Tang L, Jiang L, et al. An Effectiveness Analysis for the Multi-Factor Accelerated Test of a Copper-Free Self-Polishing Antifouling Coating. *Coatings* **2023**, *13*, 1685.
132. Lagerström M, Ytreberg E, Wiklund A-KE, Granhag L. Antifouling paints leach copper in excess—Study of metal release rates and efficacy along a salinity gradient. *Water Res.* **2020**, *186*, 116383.
133. Wang T, Chen S, Feng H, Cao L, Zhao Z, Li W. Modification strategy of siloxane antifouling coating: Adhesion strength, static antifouling, and self-healing properties. *Surf. Sci. Technol.* **2023**, *1*, 28.
134. Jiang Y, Wang K, Zhang Y, Cheng Y, Zhu T, Huang J, et al. Superoleophobic TiO_2@SSM membranes with antifouling and photocatalytic ability for efficient microbubbles flotation emulsion separation and organic pollutants degradation. *J. Membrane Sci.* **2024**, *690*, 122217.
135. Arboleda-Baena C, Osiadacz N, Parragué M, González AE, Fernández M, Finke GR, et al. Assessing Efficacy of "Eco-Friendly" and Traditional Copper-Based Antifouling Materials in a Highly Wave-Exposed Environment. *J. Mar. Sci. Eng.* **2023**, *11*, 217.
136. Dobretsov S, Abed RMM, Voolstra CR. The effect of surface colour on the formation of marine micro and macrofouling communities. *Biofouling* **2013**, *29*, 617–627.
137. Zargiel KA, Swain GW. Static vs dynamic settlement and adhesion of diatoms to ship hull coatings. *Biofouling* **2014**, *30*, 115–129.
138. Holm E, Schultz M, Haslbeck E, Talbott W, Field A. Evaluation of Hydrodynamic Drag on Experimental Fouling-release Surfaces, using Rotating Disks. *Biofouling* **2004**, *20*, 219–226.
139. Tian J, Zhao Z, Kumar A, Boughton RI, Liu H. Recent progress in design, synthesis, and applications of one-dimensional TiO_2 nanostructured surface heterostructures: A review. *Chem. Soc. Rev.* **2014**, *43*, 6920–6937.
140. Heinlaan M, Ivask A, Blinova I, Dubourguier H-C, Kahru A. Toxicity of nanosized and bulk ZnO, CuO and TiO_2 to bacteria *Vibrio fischeri* and crustaceans *Daphnia magna* and *Thamnocephalus platyurus*. *Chemosphere* **2008**, *71*, 1308–1316.
141. Jarvis TA, Miller RJ, Lenihan HS, Bielmyer GK. Toxicity of ZnO nanoparticles to the copepod Acartia tonsa, exposed through a phytoplankton diet. *Environ. Toxicol. Chem.* **2013**, *32*, 1264–1269.
142. Miller RJ, Muller EB, Cole B, Martin T, Nisbet R, Bielmyer-Fraser GK, et al. Photosynthetic efficiency predicts toxic effects of metal nanomaterials in phytoplankton. *Aquat. Toxicol.* **2017**, *183*, 85–93.